Cured of "Stickiness", Poly-L beta-Hairpin is Promoted with LL-to-DD Mutation as a Protein and a Hydrolase Mimic

ARTICLE *in* THE JOURNAL OF PHYSICAL CHEMISTRY B · DECEMBER 2010

Impact Factor: 3.3 · DOI: 10.1021/jp1062572 · Source: PubMed

Cured of "Stickiness", Poly-L β-Hairpin is Promoted with LL-to-DD Mutation as a Protein and a Hydrolase Mimic

Kirti Patel,[†] Bhupesh Goyal, Anil Kumar,[‡] Nand Kishore, and Susheel Durani*

Department of Chemistry, Indian Institute of Technology Bombay, Mumbai-400076, India

Received: July 7, 2010; Revised Manuscript Received: October 25, 2010

The planar ribbon of the poly-L β-hairpin is modified to a local ~90° bend by mutating a cross-strand pair of residues from LL to DD structure. The bend is furnished aromatic side chains in proximity of acid−base−nucleophile side chains, toward the possibility of catalyzed hydrolysis of an active-site-anchored substrate. Six sequences permuted in putative catalytic side chains are evaluated for activity and variability as hydrolase enzymes. Studies using CD, NMR, spectorofluorometry, ITC, and molecular dynamics establish that the sequences over the bent β-hairpin are by and large aggregation-free folds soluble to at least millimolar concentration, and thus remarkably contrasted with "stickiness" of the canonical poly-L β-hairpin. The heterochiral fold displays cooperative ordering and affinity for acetylcholine, *p*-nitrophenylacetate, and *p*-nitrophenylphosphate, presumably as the ligands in its aromatic pocket as a bent hairpin. The fold displays hydrolytic activity against *p*-nitrophenylacetate and manifests saturation kinetics with respect to substrate concentration. However, the catalysis power is feeble, which remains unaffected by repositioning acid−base−nucleophile side chains. Stereochemistry is proven to be critical in the balance between mutually competitive forces of polypeptide structure involved in guidance of folding or aggregation of the structure. Residue stereochemistry is confirmed in its value as the alphabet for design of protein folds to desired molecular shapes.

Introduction

The sequential codes that define proteins over the alphabet in α-amino acid structures remain poorly understood in their workings.[1−3] Proteins are approached by joining α-amino acids as defined sequences,[4−7] but the motivation remains the probing of the folding principles rather than that of harnessing their applications. In folding as conformationally well-defined structures, proteins manifest interactions that are specific for not only their chemical sequences over α-amino acid residues but also for their stereochemical sequences. Being always L in residue stereochemistry, protein polypeptides are stereochemically invariant sequences poly-L in structure. The stereochemistry defines protein folds and may determine why the folds are codable to specific molecular shapes and to specific interaction and catalytic specificities as enzymes.[8−10] Given that protein folds are defined stereochemically and that every sequence position may be set to L or D stereochemistry, the options were advocated as the alphabet to have protein shapes designed stereochemically.[11] Illustrating the concept, boat,[12] bracelet,[13] canoe,[14] and pi-cup[15] were reported as the shapes in protein structure stereospecific for L and D sequences in polypeptides that were specific in the diastereomer structures.

Since it models the β-sheet motif as an autonomous fold,[16,17] the canonical poly-L β-hairpin has allowed a critical test in protein folding of sequence effects.[17−20] The studies have enriched the understanding of protein folding and, by modeling unfolded structures,[21−23] have illuminated the aggregation of unfolded proteins as amyloids.[24,25] Given its well-defined geometry, the canonical β-hairpin was engineered as a receptor[26−29] and was exploited for nanostructure design.[30] The canonical structure is in the geometry of its flat ribbon defined with poly-L stereochemistry. The ribbon may be modified by bending its geometry without altering the ability in antiparallel strands to interact mutually, and the approach was advocated for designing folds to shapes of interest over L- and D-α-amino acids as the stereochemical alphbet.[11] Modification of stereochemistry is also promising for addressing protein-folding problems.[23,31,40] Stereochemistry determines not only how the canonical poly-L β-hairpin folds but also how it may interact within folded proteins and why it is susceptible to aggregation. Considering the geometrical role of canonical stereochemistry, the poly-L β-hairpin was guided with sequence effects to self-assembly as a C_2-symmetric dimer in side-by-side interactions over peptides of main-chain structure and as a D_2-symmetric tetramer in face-to-face assembly of the C_2 dimer over its side-chain structures.[32] In the present study, we exploit the stereochemical approach to bend the poly-L β-hairpin, which is shown, by suppressing aggregation, to promote a monomolecular fold as an autonomous protein, which we explore as an enzyme model. The synthesis and characterization of six peptides permuted in sequential placements of acid, base, and nucleophile side chains, as potential chemical catalysts of a proposed hydrolase model, are described. The sequences are shown to display on one hand cooperative ordering as proteins and on the other hand hydrolase activity of an enzyme. Stereochemistry is proven to be critical in the balance between competitive forces of polypeptide structure that specifically will direct its folding or aggregation. The alphabet in L and D structures is further proven in its value for the design of protein folds to the molecular shapes of interest.

* Corresponding author. E-mail: sdurani@iitb.ac.in. Phone: +91-22-25767164. Fax: +91-22-25767152.

[†] Present address: Department of Chemistry, RNC Arts, JDB Commerce & NSC Science College, Nashik Road-422101, India.

[‡] Present address: Department of Chemistry, University of Toronto, 80 St. George St., Toronto, ON, M5S 3H6, Canada.

10.1021/jp1062572
Published on Web 12/02/2010

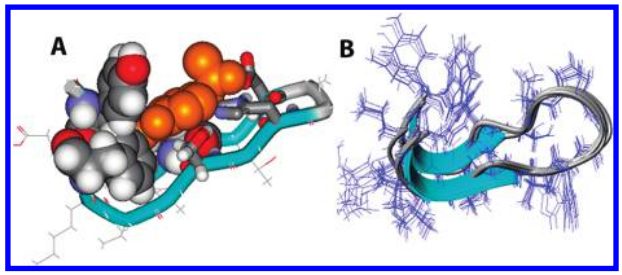

Figure 1. Canonical β-hairpin bent by LL to DD structure mutation. Panel A: *p*-nitrophenylacetate docked in the aromatic pocket has its acetyl moiety in proximity to the acid−base−nucleophile triad. Panel B: the 10 lowest energy NMR-derived structures modeled with CYANA.

Results

Design and Synthesis. The peptides 1−6 targeted in the study are titled according to their variable residues as they read from C to N terminus. Thus, with Ser (S), His (H), and Asp (D) in the sequence positions 12, 10, and 7, peptide 1 is named SHD. The peptides differ in the sequential placements of the potential catalytic triad of His, Asp, Ser, or Cys (C) residues, as is implied in the names as given below. All substituted residues are L isomers, except the residues in the sequence positions 3, 8, and 14, which are D isomers. ^{D}Pro-Gly in the sequence positions 8 and 9 defines a type II′ β-turn, which we apply as a β-hairpin nucleator.[33] The nucleated β-hairpin structure of canonical poly-L structure is modified to introduce a local bend, as noted in Figure 1A, by placing D residues in the sequence positions 3 and 14. The aromatic side chains in sequence positions 1, 5, and 16 and the acid−base−nucleophile side chains in sequence positions 7, 10, and 12 are juxtaposed for the possibility that a substrate positioned against the aromatic cluster may have an ester functionality hydrolyzable by acid, base, and nucleophilic effects of side chains.

(1) SHD:
$Ac-Y_1E_2{}^{D}L_3N_4W_5S_6D_7{}^{D}P_8G_9-H_{10}T_{11}S_{12}A_{13}{}^{D}V_{14}K_{15}F_{16}-NH_2$
(2) SHC:
$Ac-Y_1E_2{}^{D}L_3N_4W_5S_6C_7{}^{D}P_8G_9-H_{10}T_{11}S_{12}A_{13}{}^{D}V_{14}K_{15}F_{16}-NH_2$
(3) SCH:
$Ac-Y_1E_2{}^{D}L_3N_4W_5S_6H_7{}^{D}P_8G_9-C_{10}T_{11}S_{12}A_{13}{}^{D}V_{14}K_{15}F_{16}-NH_2$
(4) DHS:
$Ac-Y_1E_2{}^{D}L_3N_4W_5T_6S_7{}^{D}P_8G_9-H_{10}S_{11}D_{12}A_{13}{}^{D}V_{14}K_{15}F_{16}-NH_2$
(5) DHC:
$Ac-Y_1E_2{}^{D}L_3N_4W_5T_6C_7{}^{D}P_8G_9-H_{10}S_{11}D_{12}A_{13}{}^{D}V_{14}K_{15}F_{16}-NH_2$
(6) DCH:
$Ac-Y_1E_2{}^{D}L_3N_4W_5T_6H_7{}^{D}P_8G_9-C_{10}S_{11}D_{12}A_{13}{}^{D}V_{14}K_{15}F_{16}-NH_2$

The peptides were made by manual-solid-phase synthesis using Fmoc chemistry and displayed the expected ion peaks in QTOF-ESI MS, which are listed in Table 1 and the spectra shown in Figure S1 of the Supporting Information. HPLC on an RP-C_{18} column with H_2O (0.01% TFA)−acetonitrile 0−100% gradient established that the peptides were >95% in apparent purity.

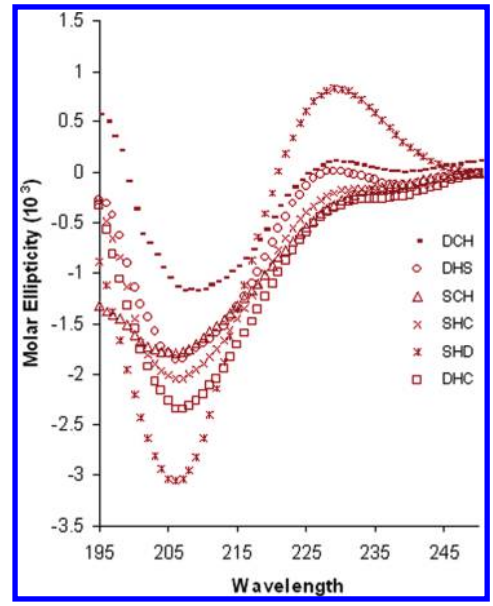

Figure 2. Apperance of a coupled exciton of aromatic chromophores in the CD spectrum.

Characterization of Conformation. In CD spectra, the peptides manifest coupled minima and maxima of ellipticity in, respectively, 208−211 and 225−240 nm range, as noted in Figure 2. The couplets manifest exciton splitting, the hallmark of interacting aromatic chromophores.[16,34] Aromatic residues characterize termini of the peptide, and hence, the peptides are folded to have the aromatic side chains interacting.

While similar in all peptides, the coupled exciton is unusually strong in the peptide SHD. Presumably, auxiliary interactions in this sequence promote stronger interactions of the aromatic side chains. Trp in position 5 displays quenched fluorescence relative to *N*-acetyltryptophanamide (NATA) as a model for isolated Trp residue. Similar in all peptides, as noted in Figure S2 of the Supporting Information, the quenching of Trp fluorescence implies that the residue could be experiencing a similar chemical environment in all sequences.

The peptides show a marginal or negligible effect of concentration on molar ellipticities of CD minima in the 40−100

TABLE 1: Analytical Data Characterizing Structures and Interactions of Hairpin Peptides

	SHD	SHC	SCH	DHS	DHC	DCH
MW_{exp} (Da)	1891	1879	1879	1891	1907	1907
MW_{obs} (Da)	1891	1879	1879	1891	1907	1907
			Conformational Stability			
melting temperature (DSC)	56.50 ± 0.65	52.67	57.13 ± 0.41	57.07 ± 1.41	67.99	58.52 ± 1.40
$\Delta G_{298\,K}$ (kJ M^{-1}) (CD)	−20.81 ± 0.23		−15.04 ± 0.45	−15.44 ± 0.41		−17.40 ± 0.45
$\Delta F_{298\,K}$ (kJ M^{-1}) (MD)	−6.23	−4.40	−9.08	−10.48	−10.90	−6.84
			Ligand Binding			
K_d (μM) (ITC)	423.00 ± 25.00	165.50 ± 15.00	90.21 ± 6.24	102.65 ± 10.99	159.68 ± 7.96	189.08 ± 15.04
$\Delta G_{298\,K}$ (kJ M^{-1}) (ITC)	−18.51 ± 1.09	−21.68 ± 1.73	−23.06 ± 0.58	−22.70 ± 1.09	−21.61 ± 0.94	−21.23 ± 0.86
ΔG (kJ M^{-1}) (AutoDock)	−16.59 ± 0.33	−18.82 ± 0.33	−17.04 ± 0.56	−17.88 ± 0.07	−20.40 ± 0.28	−16.42 ± 0.13
			Enzyme Activity			
K_M (μM)	29.84 ± 7.79	242.50 ± 13.79	87.30 ± 8.68	198.56 ± 11.25	54.26 ± 10.35	157.00 ± 15.24
K_{cat} (h^{-1})	0.54 ± 0.04	3.02 ± 0.18	0.53 ± 0.09	0.38 ± 0.05	0.58 ± 0.07	2.93 ± 0.05
K_{cat}/K_M (M^{-1} h^{-1}) (10^4)	1.81	1.24	0.61	0.19	1.07	1.87

TABLE 2: Chemical Shift Assignments of Peptide SHD

residue	NH	$C_\alpha H$	$C_\beta H$	$C_\gamma H$	others
Tyr	8.10	4.65	3.26, 3.17		7.46, 6.87
Glu	8.30	4.31	2.03, 1.90	2.30, 2.22	
^{D}Leu	8.12	4.22	1.49	1.51	0.89, 0.85
Asn	8.05	4.44	2.92, 2.80		6.98, 6.73
Trp	8.37	4.71	2.68, 2.53		7.16, 7.43, 7.06, 7.51, 7.18, 10.01
Ser	8.40	4.42	3.86, 3.80		
Asp	7.90	4.50	2.91		
^{D}Pro		4.31	2.22	1.95	3.64, 3.56
Gly	8.46	3.83			
His	8.06	4.57	3.22, 3.15		8.36, 7.16
Thr	8.36	4.39	4.22	1.17	
Ser	8.21	4.38	3.76, 3.70		
Ala	8.26	4.38	1.37		
^{D}Val	8.00	4.05	2.02	0.90	
Lys	8.51	4.17	1.56	1.17	1.56, 2.87, 7.51
Phe	8.16	4.58	3.22, 2.94		7.10, 7.33, 7.27

TABLE 3: $^3J_{NHC\alpha H}$ Values of Peptide SHD

residue	$^3J_{NHC\alpha H}$ (Hz)
Tyr(1)	7.2
Glu(2)	7.2
^{D}Leu(3)	7.2
Asn(4)	7.2
Trp(5)	7.2
Ser(6)	6.4
Asp(7)	8.0
His(10)	6.4
Thr(11)	6.4
Ser(12)	8.0
Ala(13)	6.4
^{D}Val(14)	7.2
Lys(15)	6.4
Phe(16)	8.0

μM concentration regime, as is noted in Figure S3 of the Supporting Information. In NMR, they have sharpness and chemical shifts of resonances practically unaffected upon dilution from 5.0 to 0.5 mM concentration, as is noted in Figure S4 of the Supporting Information. While showing no evidence of aggregation on this basis, the peptides were freely soluble to even higher concentrations.

Portions of TOCSY and NOESY NMR spectra of peptide 1 are shown in Figures S5 and S6 of the Supporting Information. Chemical shifts assigned with the spectra are given in Table 2. $C_\alpha H$ resonances manifest small and random chemical shift deviations with respect to random-coil values (see Figure S7 of the Supporting Information). Presumably, chemical-shift-perturbing fields of peptide dipoles are screened by the ready access of the small peptide structure to solvent.[35] $^3J_{NHC\alpha H}$ values, another diagnostic of conformation in ϕ,[36] clearly evidence the β-sheet conformation. As is noted in Table 3, all observed $^3J_{NHC\alpha H}$ values are 6 Hz or greater, as required for the β-sheet conformation.[37]

The peptide manifests a rich population of NOEs, implying close contact between the residues far off in sequence. Specifically, NOEs between Tyr(1)H^ϵ-Trp(5)$H^{\zeta 2}$, Tyr(1)H^ϵ-Trp(5)$H^{\delta 1}$, Trp(5)$H^{\delta 1}$-Phe(16)H^ϵ, Trp(5)$H^{\delta 1}$-Phe(16)H^ζ, and Tyr(1)H^δ-Phe(16)H^ζ imply close proximity of aromatic side chains. Long range NOEs appear between Trp(5)-Ser(12), Asp(7)-His(10), Asp(7)-Ser(12), ^{D}Leu(3)-^{D}Val(14), Glu(2)-Lys(15), and Ser(6)-Thr(11), which diagnose the β-hairpin fold, as is illustrated in Figure 3.

The peptide was taken up for NMR-based conformational modeling. Using NOE-based interproton distances and the $^3J_{NHC\alpha H}$-suggested range in ϕ, modeling was undertaken with CYANA-2.1.[38] Constrained with 65-intraresidue, 27-medium-ranged, and 44-long-ranged distances calibrated over NOE volumes, the modeling converged to a bent β-hairpin fold. The 10 best-fit structures superposed in Figure 1B are in mutual mean global root-mean-square deviation (rmsd) over backbone atoms, excluding N- and C-terminal residues, 0.27 ± 0.18 Å. The average NMR model, energy minimized with Gromacs,[39] has the aromatic rings in mutual geometrical modes similar to the reported consensus of geometry of the interacting stuctures;[15] specifically, Tyr(1) and Phe(16) are in edge-to-tilted (*et*) geometry, while Trp(5), Tyr(1), and Phe(16) are in offset-edge (*oe*) geometry, implying the possibility of NH−π and CH−π interactions.

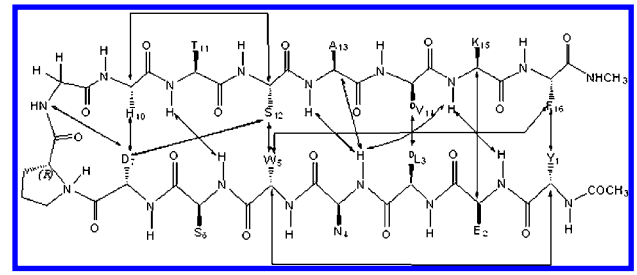

Figure 3. Schematic representation of NOEs found in the stereochemically bent β-hairpin.

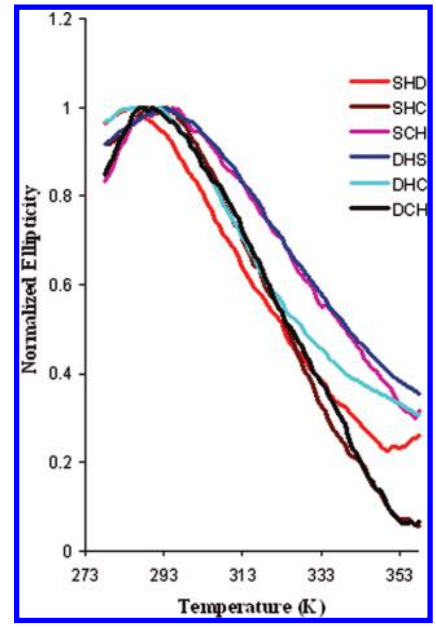

Figure 4. Temperature dependence of ellipticity is sigmoidal for several sequences.

Folding−Unfolding Equilibria. The β-hairpins were assessed for thermal unfolding with CD. According to the results in Figure 4, SHD, SCH, and DCH are sigmoidal in the melts; viz., they are two state in folding−unfolding equilibria. The other sequences do not find the higher-temperature asymptote in the melting curves. All equilibria were reversible as ≥90% of the CD signal could be recovered on cooling the melts. The results of differential scanning calorimetry (DSC) experiments are given in Figure S9 of the Supporting Information. SHD, SCH, and DCH, sigmoidal in the CD-monitored melts, are reversible in folding−unfolding transitions, as evidenced by DSC. The melts in the case of SHC and DHC are irreversible; possibly the unfolded peptides aggregate. The observed endothermic transitions may in each peptide manifest unfolding. According to the transition temperature given in Table 1, replacement of His, Asp, or Ser with Cys in position 7 destabilizes the fold.

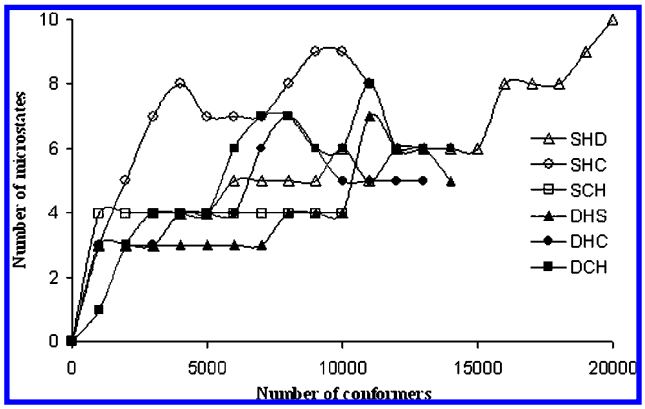

Figure 5. Evolution of population in specific folds (conformers clustered to 0.15 nm rmsd cutoff over Cα) during MD.

Computation of Conformational Equilibria. The ideal fold in each sequence was submitted to molecular dynamics in water at ambient temperature, and the trajectory was assessed for evolution of possible alternative conformational folds. The structures harvested from the molecular dynamics trajectory were clustered[55] to 0.15 nm rmsd cutoff over Cα coordinates as specific folds. Each MD trajectory is noted to evolve to an asymptote in specific conformational folds, as is noted in Figure 5. The number of folds defining apparent conformational equilibrium, ranging from 4 to 10, is sequence specific. The minimum energy conformer of each ensemble is similar to the NMR-determined conformation for SHD, as is noted in Figure 1B. The minimum energy conformer encloses 85−99% of the equilibrium in different peptides (see Figure S10 of the Supporting Information). The folding free energies, calculated by assuming two-state equilibrium, are given in Table 1. The values are noted to be in reasonable agreement with the estimates obtained with CD.

Binding with *p*-Nitrophenylphosphate. The peptides were evaluated for affinity with acetylcholine (ACh), *p*-nitrophenylacetate (pNPA), and *p*-nitrophenylphosphate (pNPP) with spectrofluorometry and isothermal titration calorimetry (ITC). On the basis of quenching of Trp fluorescence (Figure S12 of the Supporting Information), all peptides interact with all of the ligands. ACh and pNPA are comparable as quenchers, while pNPP is a stronger quencher, and also it promotes ∼30 nm red shift of the emission band. The titrations monitoring peptide−pNPA interactions with ITC are in Figure 6 and Figure S13 of the Supporting Information. The parameters derived on assuming a 1:1 binding isotherm are given in Table 1. The interactions are endothermic, and the enthalpies are in the 16−21 kJ mol^{-1} range. We evaluated the interaction with AutoDock, targeting the minimum energy fold of the SHD peptide clustered over aromatic side chains to a rmsd cutoff of 0.15 nm. The central member, energy minimized with Gromacs,[39] gave the results summarized in Table 1. The estimates are in reasonable agreement in the experimental values. According to the results of simulation, the *p*-nitrophenyl moiety binds by stacking over phenylalanine- and tryptophan-ring structures (Figure S14 of the Supporting Information).

Assessment of Catalyzed Hydrolysis. The results evaluating catalyzed hydrolysis of pNPA are in Figure S15 of the Supporting Information. An enzyme-like saturation of hydrolysis rate occurs with substrate concentration. K_M and k_{cat} given in Table 1 are narrowly varied, and k_{cat}/K_M are comparable. The intended catalytic triad does not affect the rate of substrate hydrolysis. The results of pH variation summarized in Table S2 of the Supporting Information do not evidence the participation of a titratable group in hydrolysis of the substrate. Activation consequent to binding of substrate, evidenced in the saturable kinetics, may involve electrophilic activation of the substrate.

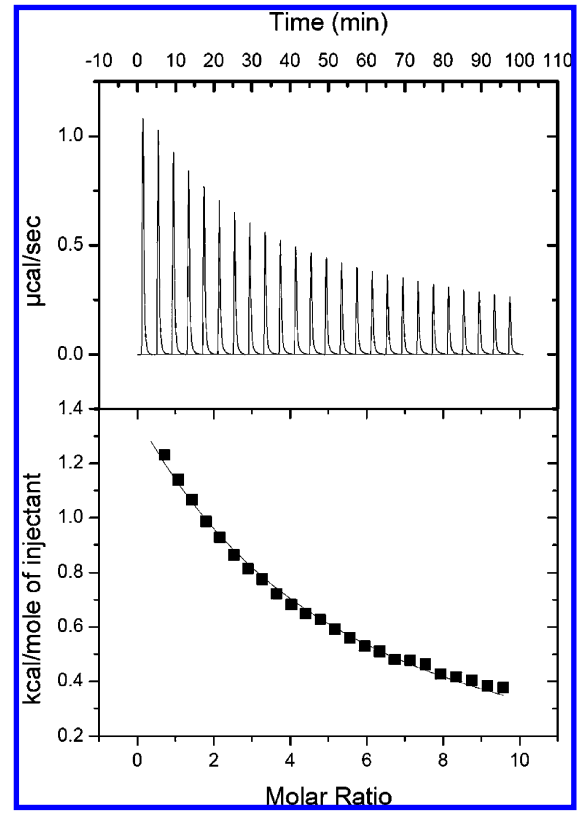

Figure 6. Interaction of SHD with *p*-nitrophenylphosphate (pNPP) monitored with ITC. Upper panel: heat changes on titrating peptide (1.4448 mL of 50 μM solution) with pNPP (10 μL aliquots of 2.5 mM solution). Lower panel: integrated heat changes in ligand titration, with the solid line representing the fit to a single binding-site model.

Discussion and Conclusions

The protein alphabet of L-α-amino acids remains an open challenge to know how it directs the specific shapes of protein structure and the specific interaction and catalysis functions of enzymes.[1−3,9] Under question are sequence effects that direct proteins as defined folds of polypeptide structure. Protein folds are specific for the poly-L diastereomer of polypeptide structure. A way to probe effects in protein folding of the interactions over the main-chain and side-chain structures, we envisioned, was to mutate the canonical structures stereochemically.[11] The mutations, transforming diastereomers, will alter molecular folds, and thus protein shapes and interactions, and thus may provide a design approach and approach to investigate folding principles. Harnessing the inverse algorithm,[41,42] we have approached homopolypeptide folds over the L and D alphabet, which we overlaid with sequences in side chains, to approach the chemical specificities of interest.[43,44] Illustrating the approach, we have in a parallel study reported a zinc-based hydrolase, which was designed first in the fold stereochemically and then in the sequence chemically.[45] Testing the systematic approach,[11−15] we targeted in this study the canonical β-hairpin for the study of L- to D-mutation effects in its shape and in its interactions as a protein and possibly as an enzyme.

The β-hairpin evokes interest in the interactions of its autonomous folding, packing as a protein element, and aggregation as an independent structure.[20,23−30] The interactions are in

the canonical structure specific for its poly-L stereochemistry. The stereochemistry defines the geometry of planar-polypeptide strands and, over their mutual hydrogen bonds, the pleated ribbons of the antiparallel-β-sheet motif. The side chains of cross-strand hydrogen-bonded and non-hydrogen-bonded residues project alternately up and down the plane of the natural poly-L ribbon.[46,47] Given its planarity, the structure can interact laterally via the array of peptide dipoles and facially via the array of side chains. The resulting main-chain and side-chain interactions, along mutually orthogonal planes, possibly provide in the β-sheet ribbon the "stickiness" in its participation either in protein folding or in amyloidogenic self-assembly of unfolded protein. Exploiting the chemical effects in self-assembly diagnosed from protein homodimers,[48] we accomplished poly-L hairpin sequences that displayed self-assembly along mutual orthogonal planes, to define a hemoglobin-like D_2 tetramer.[32]

The systematic engineering of the canonical β-hairpin to specific molecular shapes like bracelet and boat[11] has involved modifications of the structure in a cross-strand pair of LL to DD residues, which does not alter the registry of peptide hydrogen bonds but interchanges the main-chain and side-chain elements, bending the ribbon locally by about 90°. A single bend was implemented in this study, while two bends gave, based on the position along the ribbon, the curved morphology of "bracelet" and the morphology of "boat" having the ends upturned to enclose an enzyme-like pocket.[13,12] The bend was in this study examined in properties of the polypeptide structure folding as the protein and interactions as an enzyme. The canonical poly-L β-hairpin is notorious for its stickiness, and indeed, it was a challenge to design the sequences that will not aggregate and will thus allow the characterization of the structure as an autonomous fold.[16,17] We reported sequences over the poly-L hairpin structure that were dimers in the micromolar concentration regime and tetramers in the millimolar concentration regime.[32] The introduction of a single bend gave in this study a protein-like fold that is largely monomolecular and is cooperatively ordered as a protein in millimolar concentrations and presumably even higher concentrations. The suppression of stickiness of the canonical β-hairpin highlights the critical role poly-L stereochemistry may have in the trade-off in unfolded proteins between folding as specific structures and aggregating as nonspecific structures. We exploited the local bend of the heterochiral hairpin to create a pocket for enzyme-catalyzed hydrolysis of a suitable substrate. We succeeded in creating a cooperatively ordered protein-like fold, a binding pocket for a specific ligand, and rudiments of enzyme catalysis function against a substrate of interest but not the power of a real enzyme.

Experimental Section

Materials and Methods. Fmoc-protected amino acids, Rink Amide AM resin, acetylcholine, *p*-nitrophenylacetate, and *p*-nitrophenylphoshate were purchased from Sigma-Aldrich or Novabiochem-Merck.

Peptide Synthesis. Synthesis was performed manually on Rink Amide AM resin using standard Fmoc chemistry and HOBt/DIC as coupling reagents. Each coupling, monitored with Kaiser and chloranil tests, typically required about 6 h. Deprotections were carried out with 30% (v/v) piperidine−DMF. The N-terminus was acetylated ($-NHCOCH_3$) with Ac_2O:DIPEA:DMF in a 1:2:20 ratio. The cleavage of the final polypeptide and deprotection of side chains were achieved together with reagent K (82.5% TFA/5% dry-phenol/5% thioanisole/2.5% ethandithiol/5% water). The product precipitated with anhydrous diethyl ether was lyophilized from 1:4H_2O:^{t}BuOH solution as a white powder. Peptide purity was assessed with HPLC over RP-C18 (10 μM, 10 mm × 250 mm; Merck) eluting with $CH_3CN\backslash H_2O$ (0.1%TFA) 0−100% gradients.

Mass Spectra. Mass spectra were recorded on a QTOF-ESI mass spectrometer. Positive ions were detected in linear/reflectron mode.

Circular Dichroism. Circular dichroism (CD) was recorded on a JASCO J-180 CD spectropolarimeter, precalibrated with d_{10}-camphorsulphonic acid, at 298 K in a 0.2 cm path length quartz cell with 2 nm bandwidth in far-UV (190−250 nm) or near-UV (250−350 nm) range. Scanning at 100 nm/min with 1.0 s time constant, in 0.5 nm steps, five scans were averaged after baseline correction for solvent. Working solutions 20−100 μM in peptide were prepared by optical measurements. The observations in millidegrees were converted to molar residue ellipticity [θ_{MRW}] with a reported relation.[49]

Unfolding of peptides was monitored by recording the ellipticity at respective secondary CD bands in the 278−363 K range in water. The equilibrium constant was calculated as

$$K_{eq} = \frac{F_u}{1 - F_u} \tag{1}$$

where

$$F_u = \frac{[\Theta]_{obs} - [\Theta]_F}{[\Theta]_U - [\Theta]_F} \tag{2}$$

with $[\Theta]_{obs}$, $[\Theta]_F$, and $[\Theta]_U$ being the molar residue ellipticity observed, molar residue ellipticity of the folded state, and molar residue ellipticity of the unfolded state, respectively.

ΔG of the unfolding reaction was calculated as

$$\Delta G = -RT \ln K_{eq} \tag{3}$$

Spectrofluorometry. Fluorescence was measured on a Perkin-Elmer LS-55 spectrofluorimeter equipped with standard PMT. Data were collected at 298 K in a 1 mL cell, with $\lambda_{excitation}$ as 295 nm, $\lambda_{emission}$ in the 300−450 range, and 2.5 nm excitation and emission slits. A scan rate of 100 nm/min in 1 nm steps was used. The working concentrations (10−20 μM) of peptide and NATA (SIGMA chemicals) were calibrated by OD measurements using a molar extinction coefficient of Trp (∼5600 at 280 nm) and Tyr (∼1280 at 280 nm). Binding experiments were carried out at 15 μM concentration of peptide and 300 μM concentrations of pNPP, pNPA, and acetylcholine.

Nuclear Magnetic Resonance. ^{1}H NMR was measured with a Bruker 800 MHz spectrometer, equipped with a cryoprobe, at 298 K. Peptide concentrations of 5 mM were used, and 1D spectra were recorded also at 10-fold dilution. Solutions were prepared in 90% H_2O/10% D_2O with DSS as the internal reference. Polypeptide backbone and side-chain assignments were obtained with 2D ^{1}H−^{1}H TOCSY[50] experiments using a standard mlevtp pulse sequence for spin lock. A spin lock time of 90 ms was used to ensure observation of long-range couplings. The data were collected in 2k time domain points. 512 increments of t_1 were measured with 48 FIDs per increment, the data being zero-filled to 1k data points in F_1 prior to Fourier transform. Distance constraints were obtained from a 2D ^{1}H−^{1}H NOESY experiment.[51] The data were processed with TOPSPIN 2.0 and 2.1 and analyzed with Computer Aided Resonance Assignment (CARA) software. Structure calculations were

performed with CYANA 2.1.[38] Dihedral angle restraints based on $^3J_{NHC\alpha H}$ values were used, wherever possible, for structure refinements. D-Amino acid residues were introduced in the CYANA library under the guidance of the developer. Structures were energy minimized using the GROMACS software package.[39] Structural models were rendered with Pymol, MolMol, or Viewerlite software.

Isothermal Titration Calorimetry (ITC). The experiments were performed on a VP-ITC microcalorimeter (Microcal, Inc.) at 298 K. The sample cell contained peptide in 50 μM concentration, as determined by optical measurements, and the reference cell contained water. The 2.5 mM *p*-nitrophenylphosphate (ligand) solution loaded in a 250 μL syringe was titrated into peptide solution in 10 μL aliquots in 25 steps at 4 min intervals. The change in enthalpy (ΔH) due to dilution was determined by titrating ligand into solvent as well as solvent into peptide solution. These backgrounds were subtracted from ΔH obtained for the corresponding ligand−peptide binding experiments, prior to curve fitting. The background-subtracted data was fitted to a model describing a single binding site using MicroCal software. The binding enthalpy (ΔH), entropy (ΔS), and dissociation (K_d) constant were thus calculated.

Enzyme Activity. The kinetics of hydrolysis was monitored spectrophotometrically on a Perkin-Elmer spectrophotometer, fitted with peltier, using *p*-nitrophenylacetate (pNPA) as a substrate, by observing the production of *p*-nitrophenolate anion at 410 nm. A stock solution of pNPA was prepared in 20 mM sodium phosphate buffer, pH 7.0, with a few drops of acetonitrile added to solubilize the pNPA. The peptide concentration in the assays was 24 μM. Hydrolase activity was evaluated in 20 mM sodium phosphate buffer, pH 7.0, at 25 °C, by varying the substrate concentration. The catalyzed rate of pNPA hydrolysis was measured by an initial slope method, following the increase in 410 nm absorption of *p*-nitrophenolate. Errors in observation were about 5%.

Differential Scanning Calorimetry (DSC). The experiments were performed on a Mettler-Toledo DSC-822e instrument. The peptide was dissolved in water in ~40 mM concentration, and the solutions were thoroughly degassed prior to data acquisition. The sample was scanned relative to the empty aluminum pan as a reference in the temperature range 288−358 K, with a scanning rate of 5 K/min.

Molecular Dynamics. An Intel Pentium PIV Linux server, Intel Xeon dual CPU 2.4 GHz computational servers, and a PARAM Padma supercomputer equipped with 248 (Power 4@1GHz) processors and an aggregate memory of 512 GB were the hardware platforms used. Molecular dynamics was carried out in the GROMACS package[39] (versions 3.1.4, 3.2.1, 3.3.1, 3.3.2, and 3.3.3) using the gromos-96 43A1 force field[52] in a box of explicit solvent with periodic boundary conditions under NVT (constant number of particles, volume, and temperature). The nonbonded list cutoff was 1.4 nm with a shift at 0.8 nm, the integration step was 2 fs, the initial velocities were drawn from the Maxwellian distribution, and the temperature was coupled to an external bath with a relaxation time constant of 0.1 ps. Bond lengths were constrained with SHAKE[53] to a geometric accuracy of 0.0001. For an electrically charged system, counterions were added by replacing the solvent molecule to achieve electrical neutrality. First, the model peptide energy minimized was placed in a periodic cubic box of appropriate edge length and soaked in SPC water,[54] to the density in correspondence of 1 atm at 298 K. The system was energy minimized first in solvent restraining the solute and then in both solvent and the solute relieved of the restraint. Molecular dynamics was initialized, and the trajectory was sampled at intervals reported in the individual cases after allowing an initial 3 ns for equilibration.

TABLE 4: Results of Molecular Dynamics Simulation

peptide	length of simulation	no. of conformers sampled	no. of microstates recovered	% population in specific microstates 1	2	3	4	5
SHD	100	20001[a]	10	92.52	4.28	2.36	0.51	0.14
SHC	11	11001[b]	8	85.54	10.28	1.87	1.69	0.33
SCH	10	10001[b]	4	97.53	1.93	0.45	0.12	
DHS	14	14001[b]	5	98.56	0.88	0.44	0.09	0.03
DHC	13	13001[b]	5	98.81	0.86	0.25	0.08	0.02
DCH	14	14001[b]	6	94.08	3.89	1.55	0.34	0.16

[a] Conformers harvested at the 5 ps interval. [b] Conformers harvested at the 1 ps interval.

Conformational clustering to achieve microstates of peptide structure to 0.15 nm rmsd cutoff was performed with a reported procedure.[55] The difference Helmholtz free energy (ΔF_{A-B}) between specific microstates was calculated from relative probabilities p_A and p_B of finding the system in microstates A and B as $\Delta F_{A-B} = -RT \ln p_B/p_A$, with R as the gas constant, T as the temperature, and p_A and p_B the number of members in microstates A and B.

Molecular Docking. Flexible docking was implemented with AutoDock 4.0.[56] The central members of the top 10 clusters over aromatic residues of peptide conformers populating the molecular dynamics trajectory were targeted as the receptor. Using an rmsd tolerance of 2 Å, structurally distinct conformational clusters of the ligand were ranked in increasing energy.

Acknowledgment. We acknowledge DST (09DST028), Government of India, for financial support, IIT Bombay for the computing facility "Corona" and C-DAC, Govt. of India, for the supercomputing facility "BRAF". We acknowledge Dr. M. V. Hosur and Dr. Lata Panicker (BARC, Mumbai, India) for their help with DSC experiments. K.P. and B.G. are recipients of fellowships from Council of Scientific and Industrial Research (CSIR) and University Grants Commission (UGC), respectively.

Supporting Information Available: Mass, NMR, fluorescence, CD, ITC, DSC, molecular dynamics, and kinetics data. This material is available free of charge via the Internet at http://pubs.acs.org.

References and Notes

(1) Baldwin, R. L. *J. Biol. Chem.* **2003**, *278*, 17581–17588.
(2) Baldwin, R. L. *Annu. Rev. Biophys. Biomol. Struct.* **2008**, *37*, 1–21.
(3) Dill, K. A.; Ozkan, S. B.; Weikl, T. R.; Chodera, J. D.; Voelz, V. A. *Curr. Opin. Struct. Biol.* **2007**, *17*, 342–346.
(4) Kaplan, J.; DeGrado, W. F. *Proc. Natl. Acad. Sci. U.S.A.* **2004**, *101*, 11566–11570.
(5) DeGrado, W. F.; Summa, C. M.; Pavone, V.; Nastri, F.; Lombardi, A. *Annu. Rev. Biochem.* **1999**, *68*, 779–819.
(6) Razeghifard, R.; Wallace, B. B.; Pace, R. J.; Wydrzynski, T. *Curr. Protein Pept. Sci.* **2007**, *8*, 3–18.
(7) Heinisch, T.; Ward, T. R. *Curr. Opin. Chem. Biol.* **2010**, *14*, 184–199.
(8) Fersht, A. R. *Structure and Mechanism in Protein Science: A Guide to Enzyme Catalysis and Protein Folding*; W. H. Freeman and Company: New York, 1998.
(9) Schramm, V. L. *Chem. Rev.* **2006**, *106*, 3029–3030.
(10) Anfinsen, C. B. *Science* **1973**, *181*, 223–230.
(11) Durani, S. *Acc. Chem. Res.* **2008**, *41*, 1301–1308.
(12) Rana, S.; Kundu, B.; Durani, S. *Chem. Commun.* **2004**, 2462–2463.

(13) Rana, S.; Kundu, B.; Durani, S. *Chem. Commun.* **2005**, 207–209.
(14) Rana, S.; Kundu, B.; Durani, S. *Bioorg. Med. Chem.* **2007**, *15*, 3874–3882.
(15) Rana, S.; Kundu, B.; Durani, S. *Biopolymers* **2007**, *87*, 231–243.
(16) Cochran, A. G.; Skelton, N. J.; Starovasnik, M. A. *Proc. Natl. Acad. Sci. U.S.A.* **2001**, *98*, 5578–5583.
(17) Robinson, J. A. *Acc. Chem. Res.* **2008**, *41*, 1278–1288.
(18) Hughes, R. M.; Waters, M. L. *Curr. Opin. Struct. Biol.* **2006**, *16*, 514–524.
(19) Phillips, S. T.; Piersanti, G.; Bartlett, P. A. *Proc. Natl. Acad. Sci. U.S.A.* **2005**, *102*, 13737–13742.
(20) Venkatraman, J.; Shankaramma, S. C.; Balaram, P. *Chem. Rev.* **2001**, *101*, 3131–3152.
(21) Baldwin, R. L. *Adv. Protein Chem.* **2002**, *62*, 361–367.
(22) Shi, Z.; Olson, C. A.; Rose, G. D.; Baldwin, R. L.; Kallenbach, N. R. *Proc. Natl. Acad. Sci. U.S.A.* **2002**, *99*, 9190–9195.
(23) Ramakrishnan, V.; Ranbhor, R.; Durani, S. *J. Am. Chem. Soc.* **2004**, *126*, 16332–16333.
(24) Chiti, F.; Dobson, C. M. *Annu. Rev. Biochem.* **2006**, *75*, 333–366.
(25) Dobson, C. M. *Nature* **2003**, *426*, 884–890.
(26) Butterfield, S. M.; Waters, M. L. *J. Am. Chem. Soc.* **2003**, *125*, 9580–9581.
(27) Butterfield, S. M.; Goodman, C. M.; Rotello, V. M.; Waters, M. L. *Angew. Chem., Int. Ed.* **2004**, *43*, 724–727.
(28) Waters, M. L. *Biopolymers* **2004**, *76*, 435–445.
(29) Tatko, C. D.; Waters, M. L. *J. Am. Chem. Soc.* **2002**, *124*, 9372–9373.
(30) Toksoz, S.; Guler, M. O. *Nano Today* **2009**, *4*, 458–469.
(31) Kumar, A.; Ramakrishnan, V.; Ranbhor, R.; Patel, K.; Durani, S. *J. Phys. Chem. B* **2009**, *113*, 16435–16442.
(32) Pednekar, D.; Mantri, S.; Ghosh, P.; Patel, K.; Durani, S. Submitted for publication.
(33) Stanger, H. E.; Gellman, S. H. *J. Am. Chem. Soc.* **1998**, *120*, 4236–4237.
(34) Andersen, N. H.; Katherine, O. A.; Fesinmeyer, R. M.; Tan, X.; Hudson, F. M.; Eidenschink, L. A.; Farazi, S. R. *J. Am. Chem. Soc.* **2006**, *128*, 6101–6110.
(35) Avbelj, F.; Kocjan, D.; Baldwin, R. L. *Proc. Natl. Acad. Sci. U.S.A.* **2004**, *101*, 17394–17397.
(36) Karplus, M. *J. Chem. Phys.* **1959**, *30*, 11–15.
(37) Wuthrich, K. *NMR of Proteins and Nucleic Acids*; Wiley-Interscience Publication: New York, 1986.
(38) Guntert, P.; Mumenthaler, C.; Wuthrich, K. *J. Mol. Biol.* **1997**, *273*, 283–298.
(39) Lindahl, E.; Hess, B.; van der Spoel, D. *J. Mol. Model.* **2001**, *7*, 306–317.
(40) Kumar, A.; Goyal, B.; Ramakrishnan, V.; Durani, S. Submitted for publication.
(41) Das, R.; Baker, D. *Annu. Rev. Biochem.* **2008**, *77*, 363–382.
(42) Butterfoss, G.; Kuhlman, B. *Annu. Rev. Biophys. Biomol. Struct.* **2006**, *35*, 49–65.
(43) Ranbhor, R.; Tendulkar, A.; Kumar, A.; Ramakrishnan, V.; Patel, K.; Durani, S. Submitted for publication.
(44) Ranbhor, R.; Kumar, A.; Patel, K.; Ramakrishnan, V.; Durani, S. Submitted for publication.
(45) Patel, K.; Srivastava, K. R.; Durani, S. *Bioorg. Med. Chem.* [Online early access]. DOI: 10.1016/j.bmc.2010.10.003. Published Online: Oct 10, **2010**.
(46) Branden, C.; Tooze, J. *Introduction to Protein Structure*; Garland Publishing Inc.: New York, 1999.
(47) Cantor, C. R.; Schimmel, P. R. *Biophysical Chemistry*; W. H. Freeman: New York, 1980.
(48) Pednekar, D.; Durani, S. *Proteins.*, in press.
(49) Creighton, T. E. *Protein Structure: A practical approach*; IRL Press: Oxford, U.K., 1989.
(50) Davis, D. G.; Bax, A. *J. Am. Chem. Soc.* **1985**, *107*, 2820–2821.
(51) Kumar, A.; Ernst, R. R.; Wuthrich, K. *Biochem. Biophys. Res. Commun.* **1980**, *95*, 1–6.
(52) van Gunsteren, W. F.; Billeter, S. R.; Eising, A. A.; Hunenberger, P. H.; Kruger, P.; Mark, A. E.; Scott, W. R. P.; Tironi, I. G. *Biomolecular Simulation: The GROMOS96 Manual and User Guide*; Hochschulverlag AG and the ETH Zurich: Zurich, Switzerland, 1996.
(53) Ryckaert, J. P.; Ciccoti, G.; Berendsen, H. J. C. *J. Comput. Phys.* **1977**, *23*, 327–341.
(54) Berendsen, H. J. C.; Postma, J. P. M.; van Gunsteren, W. F.; Hermans, J. *Interaction models for water in relation to protein hydration. Intermolecular Forces*; Pullman, B. Ed.; Reidel Publishing Company: Dordrecht, The Netherlands, 1981; pp. 331−342.
(55) Daura, X.; Gademann, K.; Jaun, B.; Seebach, D.; van Gunsteren, W. F.; Mark, A. E. *Angew. Chem., Int. Ed.* **1999**, *38*, 236–240.
(56) Morris, G. M.; Huey, R.; Lindstrom, W.; Sanner, M. F.; Belew, R. K.; Goodsell, D. S.; Olson, A. J. *J. Comput. Chem.* **2009**, *30*, 2785–2791.

JP1062572